The Journal of Neuroscience, September 1994, 14(9): 5160–5169

Spatial and Temporal Expression Patterns of Two Sodium Channel Genes in *Drosophila*

Chang-Sook Hong and Barry Ganetzky

Laboratory of Genetics, University of Wisconsin, Madison, Wisconsin 53706

Genetic and molecular studies have identified two different sodium channel genes in *Drosophila*, *para* and *DSC1*. The functional contributions of the *para*-encoded channel have been inferred from analysis of mutant phenotypes. However, no mutations of *DSC1* have been identified, so the *in vivo* functions of the channel it encodes are not yet known. To learn more about the possible functions of *DSC1* in the *Drosophila* nervous system compared with those of *para*, we have characterized the expression patterns of these two sodium channel genes at embryonic, larval, pupal, and adult stages by tissue *in situ* hybridization. *para* encodes the predominant type of sodium channel and is ubiquitously transcribed throughout the CNS and PNS at all developmental stages. The expression pattern of *DSC1* is very different from *para* during embryonic and larval stages during which there are very few *DSC1*-expressing cells in either the CNS or PNS. Double-labeling studies suggest that some of these cells are non-neuronal. However, in pupal and adult stages, *para* and *DSC1* have completely overlapping patterns of expression in the CNS and retina. In the pupal and adult, PNS expression of these genes is still distinct because only *para* transcripts are detected in wing sensory neurons. The strong and widespread expression of *DSC1* in the CNS of pupae and adults suggests that the *DSC1* channels are likely to provide an important function in neurons during these stages. Since most, if not all, neurons in the pupal and adult CNS express both *para* and *DSC1*, these two sodium channel genes probably subserve distinct functions within these cells. Our results provide the background for elucidating the respective *in vivo* contributions of *para* and *DSC1* to neuronal excitability and for dissecting the regulatory mechanisms that underlie their different patterns of expression.

[Key words:* Drosophila, para, DSC1, *sodium channel, gene expression,* in situ *hybridization]

The electrical properties of a neuron are largely shaped by the types and relative abundance of ion channels that are expressed. Generally, ion channel genes are members of families in which two or more genes encode channels with similar, but not identical, functional properties (Hille, 1992). The signaling capabilities of a given neuron may vary, depending on which member of an ion channel family is expressed. For example, in mammals, at least five genes encode sodium channel polypeptides, three of which are expressed in neurons and two in skeletal muscle (Noda et al., 1986; Kayano et al., 1988; Rogart et al., 1989; Trimmer et al., 1989; Kallen et al., 1990). Each of these genes has a distinctive temporal and spatial pattern of expression, resulting in distributions of sodium channel types that are largely nonoverlapping (reviewed by Mandel, 1992). Thus, in rat brain the mRNA levels of neuronal sodium channel types II and III increase during neurogenesis from embryonic day 10 to birth. Type II mRNA levels remain high in adults, whereas type III decreases to a lower level. Type I mRNA does not show appreciable abundance until birth. The type II and type III genes are expressed throughout the CNS, but only sparsely in the PNS. Expression of the type I gene is most abundant in caudal regions of the brain and in the spinal cord. The implication from the existence of this family of sodium channel genes, each with its own pattern of expression, is that the different sodium channel polypeptides have distinctive functional properties that are important in determining the characteristic firing properties of a particular type of neuron. However, it has not yet been possible experimentally to determine the respective functional contributions of each sodium channel type to the electrophysiological properties of the neurons in which they are expressed.

Because of the numerous genetic and molecular tools available, *Drosophila* is well suited for investigating problems of this type. At least two different sodium channel structural genes have been identified in *Drosophila*. The *para* (paralytic) locus was first identified on the basis of mutations causing a temperature-sensitive paralytic phenotype (Suzuki et al., 1971; Siddiqi and Benzer, 1976). Electrophysiological experiments demonstrated that paralysis was correlated with a temperature-dependent block in the propagation of neuronal action potentials (Siddiqi and Benzer, 1976; Wu and Ganetzky, 1980). Subsequently, molecular analysis of this gene revealed that it encoded a sodium channel polypeptide sharing about 60% amino acid identity with rat brain sodium channels (Loughney et al., 1989; Ramaswami and Tanouye, 1989). Another presumptive sodium channel gene, *DSC1* (*Drosophila* sodium channel), was cloned on the basis of its homology to vertebrate sodium channel probes (Salkoff et al., 1987; Ramaswami and Tanouye, 1989). The importance of the *DSC1* channel to neuronal excitability is not known because mutations affecting its function have not yet been isolated. However, the extensive sequence divergence between *para* and *DSC1* suggests that the encoded polypeptides may have distinct physiological functions in the *Drosophila* nervous system. However,

Received Dec. 20, 1993; revised Mar. 16, 1994; accepted Mar. 24, 1994.

We thank Jon Karpilow, Janna McLean, Richard Ordway, and Justin Thackeray for comments on the manuscript and members of Mike Hoffmann's laboratory for advice and help with *in situ* hybridization and histological techniques. This work was supported by National Institutes of Health Grant GM43100. This is paper 3393 from the Laboratory of Genetics, University of Wisconsin, Madison.

Correspondence should be addressed to Dr. Barry Ganetzky, Laboratory of Genetics, 445 Henry Mall, University of Wisconsin, Madison, WI 53706.

only limited characterization of the expression of these genes in pupae and adults has been reported (Tseng-Crank et al., 1991; Amichot et al., 1993), so it is not yet known whether the two *Drosophila* sodium channel types are differentially distributed in the nervous system throughout development. To study the expression of these genes in detail, we have used tissue *in situ* hybridization to characterize their spatial and temporal pattern of transcription from embryonic through adult stages. Our results demonstrate that *para* is ubiquitously expressed throughout the CNS and PNS at all developmental stages. In contrast, *DSC1* has a restricted pattern of expression in embryos that shows little, if any, overlap with *para*. Surprisingly, however, there is almost complete overlap in the expression of *para* and *DSC1* in the CNS of pupae and adults. These results provide the background for assessing the respective *in vivo* contributions of *para* and *DSC1* to neuronal excitability and for elucidating the regulatory mechanisms that underlie their different patterns of expression.

Materials and Methods

Fly stocks. Drosophila melanogaster were raised on standard *Drosophila* medium at 25°C. The wild-type strain used in all experiments was Canton Special (*CS*). The null mutation *para*^{lk2} has been previously described (Loughney et al., 1989) and was used as a negative control for the specificity of the *para in situ* probes.

Hybridization probes. A mixed probe synthesized from three DNA templates was used for detection of *para* transcripts: the 0.29 kb EcoRI-BamHI fragment of cDNA ZS10.3, the 0.69 kb BglI-ClaI fragment of cDNA ZS10.3, and the 1.0 kb EcoRI-MspI fragment of cDNA GS12.1 (Loughney et al., 1989). These cDNA fragments encoded the cytoplasmic domains of the amino terminus and the linking regions between the first and second or second and third homology domains of the *para* polypeptide. These regions show no conservation between the *para* polypeptide and other known sodium channel polypeptides. Except for the 24 nucleotide segment corresponding to alternative exon b present in the 0.69 kb BglI-ClaI fragment, all templates contained exon sequences common to all *para* transcripts (Loughney et al., 1989). Templates for synthesis of *DSC1* probes were either the 1.7 kb cDNA B1, which encodes the region distal to the third homology domain of the *DSC1* polypeptide (Ramaswami and Tanouye, 1989), or a PCR-amplified fragment that corresponds to the first cytoplasmic linking region. Identical results were obtained with either probe. Digoxigenin-labeled DNA probes were synthesized by random priming according to manufacturer's instructions (Genius kit, Boehringer-Mannheim). In some experiments, increased sensitivity was obtained by using digoxigenin-labeled single-stranded RNA probes. RNA probes were made by *in vitro* transcription according to manufacturer's instructions (Boehringer-Mannheim).

In situ *hybridization.* Nonradioactive *in situ* localization of RNA in whole embryos was done as described by Tautz and Pfeifle (1989) and Masucci et al. (1990) with some modifications. Embryos (0–16 hr) were prefixed by shaking for 20–30 min in heptane saturated with 10% formaldehyde, PBS (PBS = 10 mM KPO_4, 140 mM NaCl, pH 7.2), 50 mM EGTA. To devitellinize the embryos the aqueous phase and most of the heptane were removed, methanol was added, and the embryos were shaken vigorously for several minutes. The embryos were then rinsed with methanol and then with 100% ethanol several times and stored at −20°C. Embryos were rehydrated by rinsing once in 50% ethanol, 50% PBT (PBT = PBS + 0.1% Tween) and then three times in PBT. Following rehydration, embryos were fixed for 15 min on ice in 5% formaldehyde, PBS, and then for 15 min at room temperature in 5% formaldehyde, PBT. Fixed embryos were treated with proteinase K, washed, prehybridized, hybridized, and washed as described in Tautz and Pfeifle (1989). Hybridization was done for 24–36 hr at 48°C for DNA probes and at 55°C for RNA probes. Embryos were incubated with preabsorbed alkaline phosphatase-conjugated antidigoxygenin antibody, diluted 1:2000, for 1 hr at room temperature. After color development, embryos were mounted in glycerol or dehydrated in ethanol and then mounted in methyl salicylate.

Larval brain and imaginal discs were dissected out in PBS before fixing in 5% formaldehyde, PBS. Pupal heads and wings from 25 hr pupae were dissected out from the pupal case and cuticular membrane and then fixed in 5% formaldehyde, PBS. Dissected tissues were hybridized *in situ* by the same procedures as described above for embryos. After the color reaction, larval ganglia and pupal heads were dehydrated in ethanol and cleared and mounted in methyl salicylate and then embedded in plastic resin (Ernest Fullam and Co.) as described by Reuter and Scott (1990). After overnight polymerization, the tissues were sectioned at 4 μm thickness with an ultracut microtome using glass knives.

Heads from 72 hr pupae and adults were frozen in Tissuetek O.C.T. compound (Lab-Tek Division, Miles) on a block of dry ice and then sectioned at 10 μm thickness using a cryostat. Most procedures following sectioning were modified from a protocol designed for radioactive probes (Hafen and Levine, 1986). Tissue sections were fixed, treated with pronase, and prehybridized as described by Hafen and Levine (1986). Hybridization with digoxigenin-labeled RNA or DNA probes was carried out for 18–24 hr at 45°C in a moist chamber. After hybridization, the slides were washed five times for 10 min each in 2× SSC (SSC = 0.15 M NaCl, 0.015 M Na-citrate), twice in 1× SSC, and twice in 0.5× SSC at 45°C. Color development was as described for whole embryos. After staining, the slides were dehydrated through an ethanol/xylene series and mounted with Permount.

Double labeling with anti-HRP immunohistochemistry. After *in situ* hybridization as described above, embryos were incubated for 1 hr with anti-HRP antibody (Sigma; diluted 1:200), washed, and incubated for 1 hr with horseradish peroxidase–conjugated goat anti-rabbit IgG (Sigma; diluted 1:500). Detection was done according to manufacturer's recommendations. After color development, embryos were mounted in 90% glycerol and the ventral nerve cord and the PNS were dissected out for flat mounting.

Results

Embryonic expression patterns of para *and* DSC1 *are different*

During *Drosophila* neurogenesis, neuroblasts begin to segregate from the ectoderm at the beginning of stage 9 and undergo asymmetric division to generate ganglion mother cells. In turn, these cells divide symmetrically to produce pairs of postmitotic neurons through stage 12 (Campos-Ortega and Hartenstein, 1985; Campos-Ortega and Jan, 1991). We used a *para* cDNA restriction fragment as a probe for tissue *in situ* hybridization to examine expression of *para* transcripts in the developing nervous system. In whole-mount embryos *para* expression is not observed prior to stage 12 but becomes detectable after early stage 13 (Fig. 1*A,C*). By using genomic DNA probes corresponding to the 5′ untranslated leader, *para* transcripts could be detected at late stage 12, about 50 min earlier (data not shown) than with probes derived from the translated region. Thus, transcription of *para* probably initiates during late stage 12 in neurons but not in neuroblasts.

At stage 13, *para* transcripts are detected in the ventral nerve cord and in the antennomaxillary complex. Besides the neurons in the antennomaxillary complex, only a few other cells in the peripheral nervous system (PNS) show any *para* expression at this time. Because sensory neurons develop sequentially in *Drosophila* and only a few are present by stage 13 (Hartenstein, 1988), the stained cells in the periphery probably include the first sensory neurons to appear. Development of the PNS is complete by stage 15, at which time most, and perhaps all, sensory neurons express *para* (Fig. 1*E*). In the CNS, the *para* transcript is detected continuously and strongly from stage 13 onward (Fig. 1*C,G*). Antibodies to horseradish peroxidase (HRP) recognize most neuronal cell bodies and axon tracts in the *Drosophila* nervous system (Jan and Jan, 1982). Double labeling experiments using anti-HRP antibodies in addition to probes for the *para* transcript were carried out to confirm the neuronal identity of *para*-expressing cells and to determine the location of these cells relative to axon tracts. As shown in Figure 2, *A* and *B*, there are clusters of *para*-expressing neurons near the

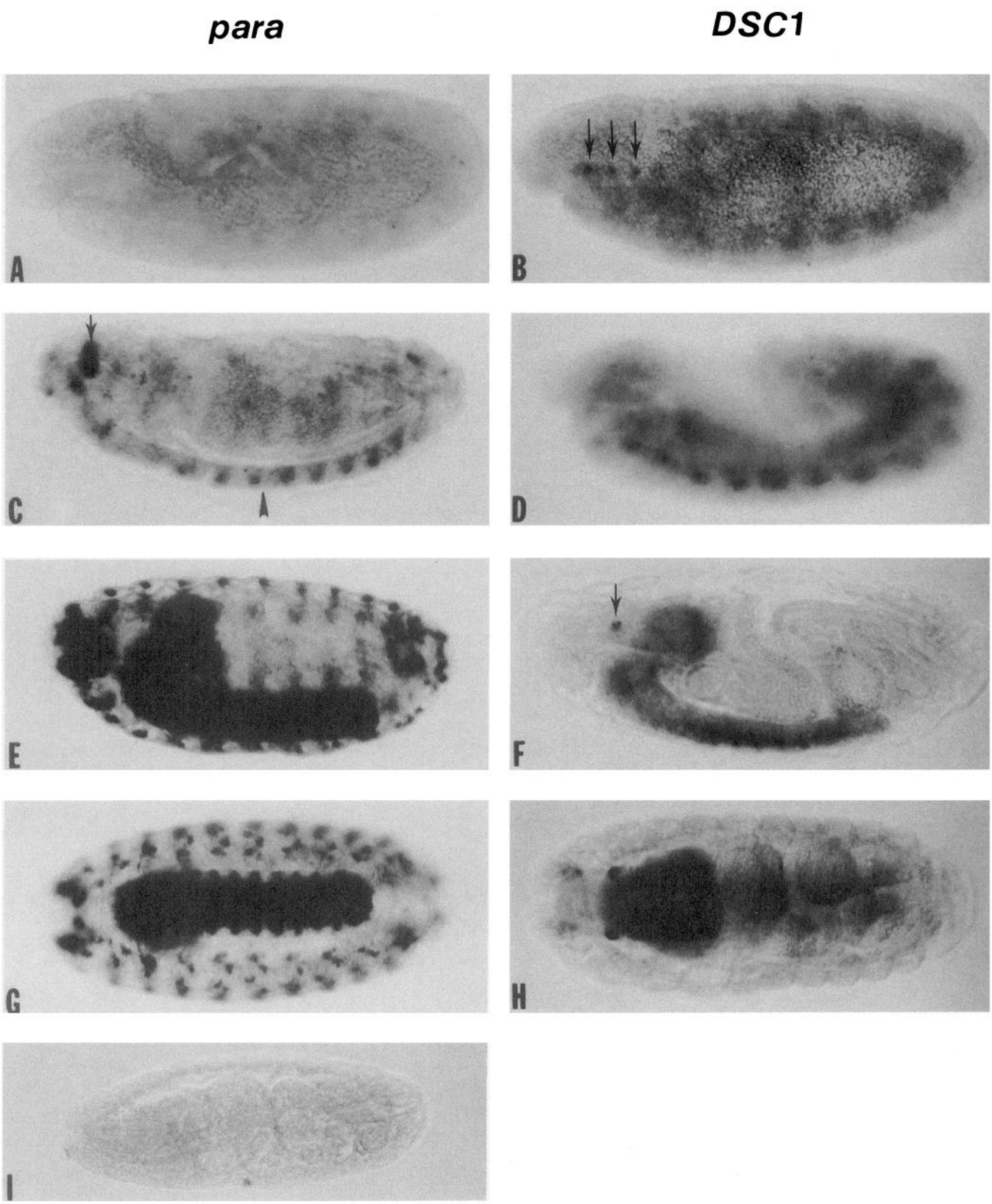

Figure 1. Analysis of embryonic expression of *para* and *DSC1* sodium channel genes by *in situ* hybridization. *Left panels* (*A, C, E, G,* and *I*) show *para* expression, and *right panels* (*B, D, F,* and *H*), *DSC1* expression. *A–F* are lateral views of wild-type embryos of various stages. The embryos are oriented with anterior to the left and ventral down. *A,* Stage 12 embryo hybridized with *para* probe. No detectable staining is seen. *B,* Stage 12 embryo hybridized with *DSC1* probe. Expression can be observed in some cells in the developing stomatogastric ganglion (*arrows*) and germ band. *C,* Stage 13 embryo hybridized with *para* probe. Staining is present in the antennomaxillary complex (*arrow*) and ventral nerve cord (*arrowhead*). *D,* Late stage 12 embryo hybridized with *DSC1* probe. Staining appears in segmentally repeating cells along the ventral cord. *E,* Stage

midline and at the lateral margins of the CNS close to the posterior commissures in every segment. In addition, double labeling experiments in the PNS indicate that the group of neurons expressing the HRP antigen is indistinguishable from the *para*-expressing cells (Fig. 2*E,F,H*). Thus, by stage 17, the final stage of embryonic development, *para* appears to be expressed in most, if not all, neurons in both the CNS and PNS.

To confirm the specificity of the probes for the *para* transcript, *in situ* hybridization was carried out on embryos produced by *FM7/para*^{lk2} mothers. The *para*^{lk2} allele is a null mutation associated with an inversion breakpoint within the open reading frame of *para* (Loughney et al., 1989). The majority of *para*^{lk2} homozygous embryos have been found to survive through embryogenesis until hatching (unpublished observations). When *FM7/para*^{lk2} females are crossed to *FM7/Y* males, about 25% of the resulting embryos should be *para*$^{lk2/Y}$ mutant males and fail to express the *para* transcript. Examination of 141 late stage embryos from this cross revealed 34 (24%) that did not hybridize with the *para* probes (Fig. 1*I*), demonstrating the specificity of the probes for the *para* transcript.

DSC1 is first detected somewhat earlier than *para* at early stage 12 prior to germ band retraction (Fig. 1*B*). At this stage, several *DSC1*-expressing cells appear in the dorsal wall of the foregut. The position of these cells appears to correspond to that of the stomatogastric nervous system, which gives rise to the frontal and parapharyngeal ganglia during stage 15 (Campos-Ortega and Hartenstein, 1985). By late stage 15, *DSC1* expression is prominent in the frontal ganglionic region (Figs. 1*F,H*; 2*I*). Elsewhere in the PNS, some scattered *DSC1*-expressing cells (Fig. 2*G,I*) can be observed that are difficult to identify. A highly reproducible pattern occurs in the abdominal segments where a single *DSC1*-expressing cell is present immediately ventral to every lateral chordotonal organ. Because these cells are anti-HRP negative, their identity as sensory neurons is uncertain.

In the CNS, *DSC1* expression is detected during germ band retraction as a single cluster per segment along the ventral nerve cord (Fig. 1*D*). By stage 15, *DSC1* is expressed in a regular pattern in some cells located along the longitudinal commissures of the CNS, as revealed by double labeling with anti-HRP (Fig. 2*C,D*). In abdominal segments A1–A7, a pair of *DSC1*-expressing cells lies between the anterior and posterior commissures, very close to the longitudinal commissures and dorsal to the *para*-expressing neurons. This pattern was not evident in the thoracic segments or in the terminal abdominal segment. Although it is difficult to determine their exact identity, the location of these *DSC1*-expressing cells suggests they could correspond to longitudinal glia (Klambt and Goodman, 1991).

The results of these *in situ* hybridization experiments indicate that *para* and *DSC1* are expressed in different subsets of cells in the embryonic CNS and PNS.

Differential expression of para *and* DSC1 *continues through the larval stage*

We examined whether the differential expression of *para* and *DSC1* continues through later developmental stages. *In situ* expression patterns of *para* and *DSC1* were studied in third instar larvae using whole-mounts or plastic sections. Expression of *para* was detected in larval brain, ventral ganglia, eye disc, and leg disc (Fig. 3). In each brain hemisphere, *para* is expressed in the cellular cortical region and in the developing medullar and laminar regions of the visual system (Fig. 3*A*). The inner and outer proliferation centers of the optic lobes, which consist of clustered neuroblasts (White and Kankel, 1978) do not exhibit *para* expression. In the ventral ganglion, *para* expression occurs in a segmentally repeated pattern that includes medial, ventrolateral, and dorsolateral neurons (Fig. 3*C*). This staining pattern appears to reflect the continued expression of *para* in embryonically derived neurons. The vast majority of cells in the ventral ganglion of third instar larvae are produced by larval neuroblasts that undergo mitotic activity throughout larval development (Truman and Bate, 1988). The progeny cells, which will form the adult ventral CNS, accumulate in an immature, arrested state that do not differentiate into mature neurons until metamorphosis. No detectable expression of *para* is found in these postembryonically derived neuronal precursors before pupal development. Thus, expression of *para* in the larval CNS is limited to mature neurons that regulate the behavior of the larva.

In leg discs, several *para*-expressing cells are detected near the larval nerve that connects the disc with the CNS (Fig. 3*D*). These cells appear to be larval sensory neurons, which are born early during embryogenesis (Jan et al., 1985; Tix et al., 1989). Expression of *para* is also detected in the developing eye imaginal disc (Fig. 3*E*). During the third larval instar, development of ommatidia begins within the morphogenetic furrow as it advances across the disc in a posterior-to-anterior direction (Ready et al., 1976). Randomly arranged undifferentiated cells are located anterior to this furrow. Cellular differentiation and the ordered assembly of cell clusters in each ommatidium begin posterior to the furrow (Ready et al., 1976). Immediately posterior to the furrow, preclusters containing five photoreceptor cells are formed. A second wave of mitosis following the furrow gives rise to three other photoreceptor cells, which are added to the preclusters to form clusters of eight photoreceptors. Posterior to the second mitotic wave, a group of *para*-expressing cells, corresponding to the developing photoreceptors, can be seen in each ommatidium. However, little or no *para* expression is detectable in the most posterior part of the eye disc. Thus, *para* expression appears to diminish as the ommatidial clusters mature further and remains off until late pupal stages (see below).

No *para* expression is evident in the other imaginal discs, indicating that sensory neurons in these discs may not yet be present. This agrees with the observation that sensory neurons in the wing and haltere discs appear only after the onset of metamorphosis (Tix et al., 1989; Huang et al., 1991).

There is no detectable expression of *DSC1* in the ventral ganglion or imaginal discs in third instar larvae (data not shown). In the brain, the only detectable expression of *DSC1* is in the laminar region of the optic lobes (Fig. 3*B*) where it appears to be even more abundantly expressed than *para*. Although it is difficult to make quantitative comparisons of gene expression on the basis of tissue *in situ* hybridization, the reproducibility

←

16 embryo hybridized with *para* probe. Strong expression is seen in the antennomaxillary complex and throughout the entire PNS and CNS. *F*, Stage 16 embryo hybridized with *DSC1* probe. Some expression is detected in the CNS and frontal ganglion (*arrows*) but only faintly elsewhere in the PNS. *G* and *H* are ventral views of stage 16 wild-type embryos oriented with anterior to the left. *G*, Hybridization with *para* probe. *H*, Hybridization with *DSC1* probe. *I*, Lateral view of stage 16 *para*^{lk2} embryo hybridized with *para* probe. Staining is absent in the mutant embryo.

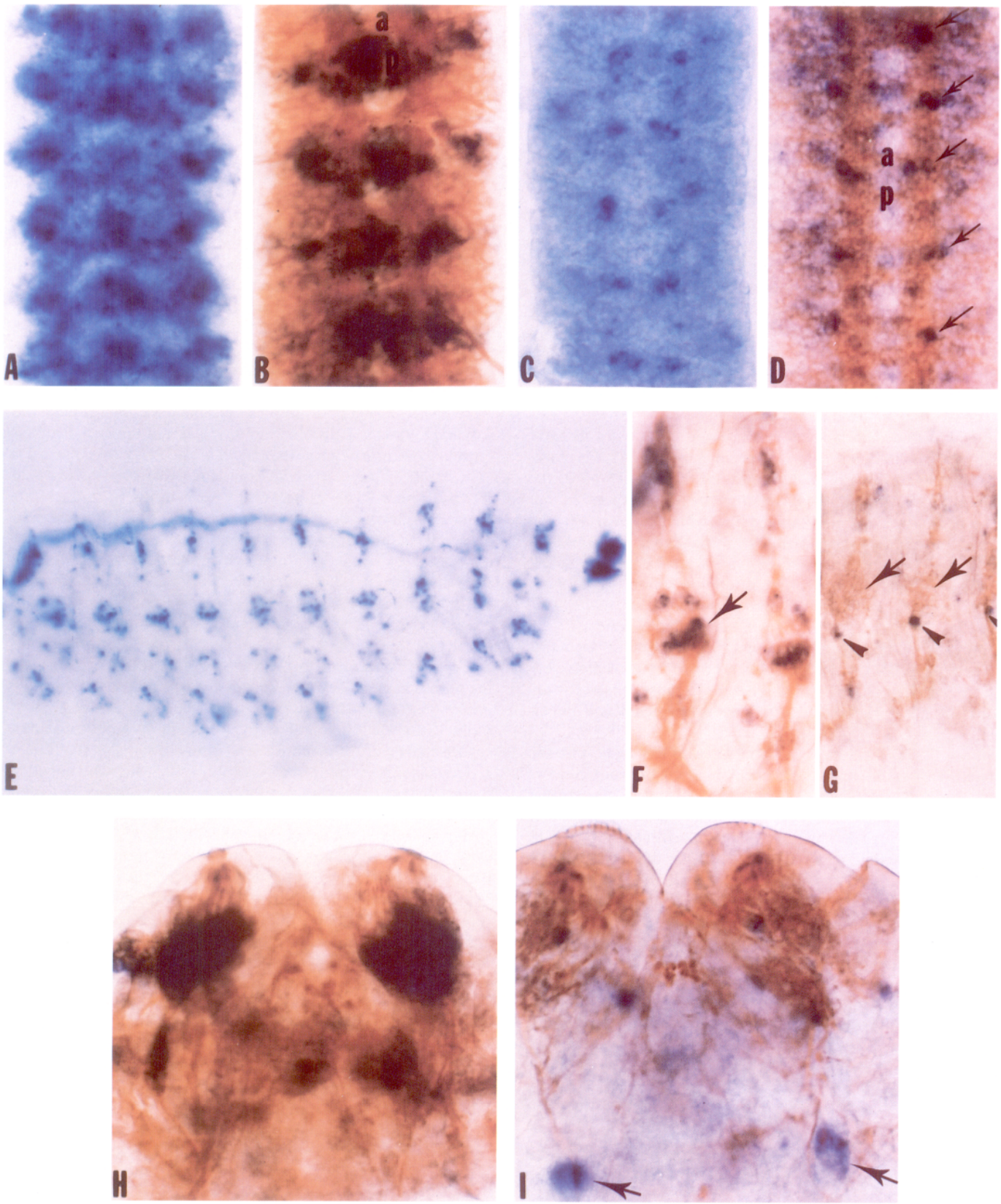

Figure 2. Higher-resolution analysis of *para*- and *DSC1*-expressing cells in the embryonic CNS and PNS by *in situ* hybridization and double labeling with anti-HRP antibodies. *A–D* show ventral views of expression in ventral ganglion dissected from stage 17 embryos oriented with anterior toward the top. *A, In situ* hybridization with *para* probe. *B,* Double labeling: *in situ* hybridization with *para* probe and immunostaining with anti-HRP antibody (*brown color*) to show location of *para*-expressing cells relative to axonal tracts. The anti-HRP antibody highlights the longitudinal and anterior (*a*) and posterior (*p*) transverse commissures. These axon tracts run between the cell clusters showing strong staining for the *para*

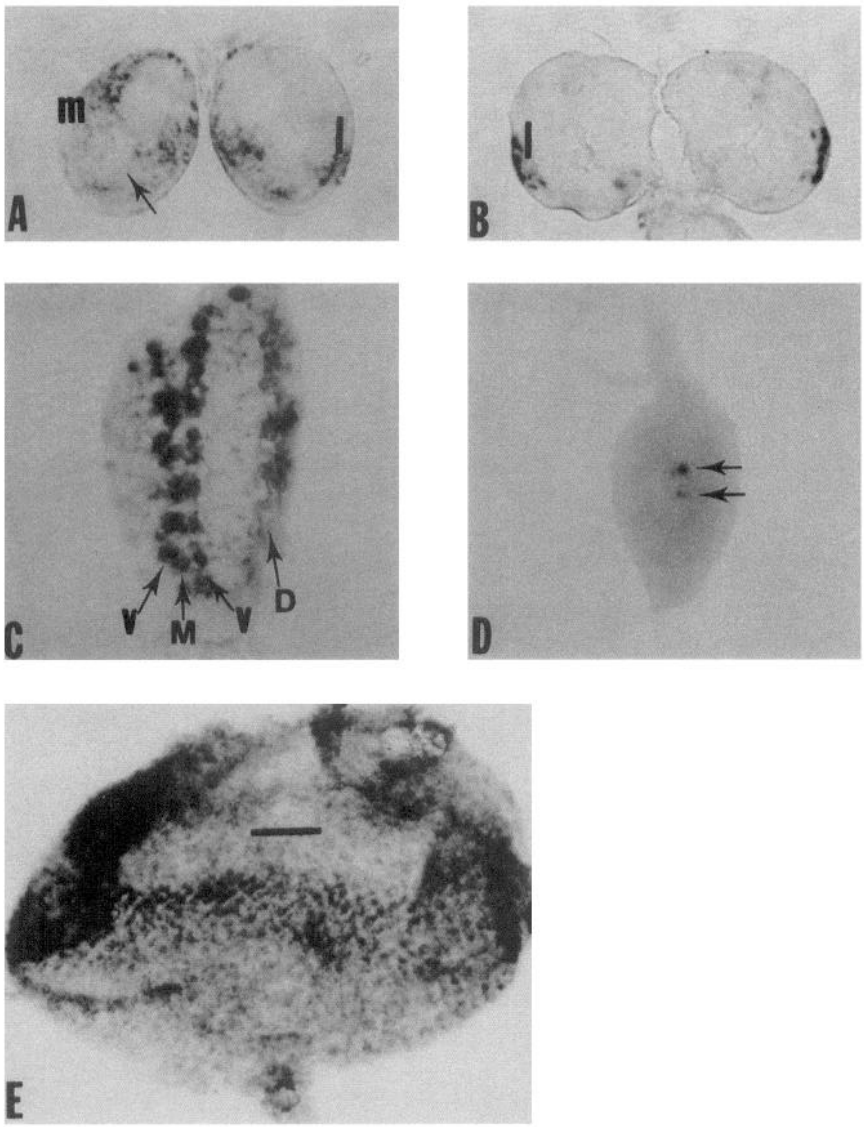

Figure 3. Comparison of *para* and *DSC1* expression in third instar larvae. *A–C* are horizontal sections through the larval brain and ventral ganglion at about midlevel. Anterior is up. *A* and *C*, Expression of *para* in the larval brain hemispheres and the ventral ganglion. Expression is detected in the cortical region and developing laminar (*l*) and medullar region (*m*). The inner and outer proliferation centers (*arrow*) show no staining. In the ventral ganglion, *para* expression is seen in medial (*M*), ventrolateral (*V*), and dorsolateral (*D*) neurons. *B*, Expression of *DSC1* in brain hemispheres. Note prominent expression in the developing laminar region (*l*). *D*, *para* expression (*arrows*) in the leg disc and *E*, in eye disc whole-mount *in situ* hybridized. *Short line* marks the morphogenetic furrow. Posterior is down. Note the faint staining in the very posterior region of eye disc.

of the intense *DSC1* staining in the lamina suggests that this is one region where its expression is at higher levels than *para*. As in embryos, there is little overlap between *para* and *DSC1* expression in the larval nervous system.

Overlapping expression patterns of para *and* DSC1 *in early pupae*

Expression of *para* and *DSC1* was examined in the pupal nervous system beginning at 25 hr after pupariation. At this stage, *para* transcripts are detected throughout the cellular cortex of the brain, in antennal neurons and also in the optic lobes (Fig. 4*A*). By this stage, the visual system has developed highly ordered structures in which visual information will undergo serial processing (Kankel et al., 1980). The R1 through R6 photoreceptors terminate in the lamina from which laminar neuropil extends to the medulla. The R7 and R8 photoreceptors synapse directly in the medulla. Neurons in the medulla form synaptic connections in the lobula and lobular plate. Expression of *para* is detected throughout the cortices of the lamina, medulla, and lobula complex. However, no significant signal is detectable in the retinal region. In young pupae the retina is not differentiated completely and is very thin. Later, about 72 hr after pupariation,

←

transcript. *C*, *In situ* hybridization with *DSC1* probe. *D*, Double labeling: *in situ* hybridization with *DSC1* probe and immunostaining with anti-HRP antibody. *DSC1*-expressing cells (*arrows*) are located along the longitudinal commissures close to the anterior transverse commissures. *E–G* show lateral views of expression in the PNS of stage 17 wild-type embryos oriented with anterior to the left and ventral down. *E*, *In situ* hybridization with *para* probe. *F*, Double labeling: *in situ* hybridization with *para* probe and immunostaining with anti-HRP antibody. There is good correspondence between the *para*-expressing cells and those stained with the anti-HRP antibody. For comparison with *DSC1* expression in *G* below, note expression of *para* in the chordotonal organ (*arrow*). *G*, Double labeling: *in situ* hybridization with *DSC1* probe and immunostaining with anti-HRP antibody. Few or none of the cells stained with the anti-HRP antibody have detectable levels of *DSC1* expression. A *DSC1*-expressing cell (*arrowhead*), which is not stained with the antibody, is located ventral to every lateral chordotonal organ (*arrows*). *H*, Colabeling of *para*-expressing cells with anti-HRP antibody in the antennomaxillary complex. Anterior is up. Dorsal focus. *I*, Expression of *DSC1* in the frontal ganglion (*arrows*). Double labeling: *in situ* hybridization with *DSC1* probe and immunostaining with anti-HRP antibody.

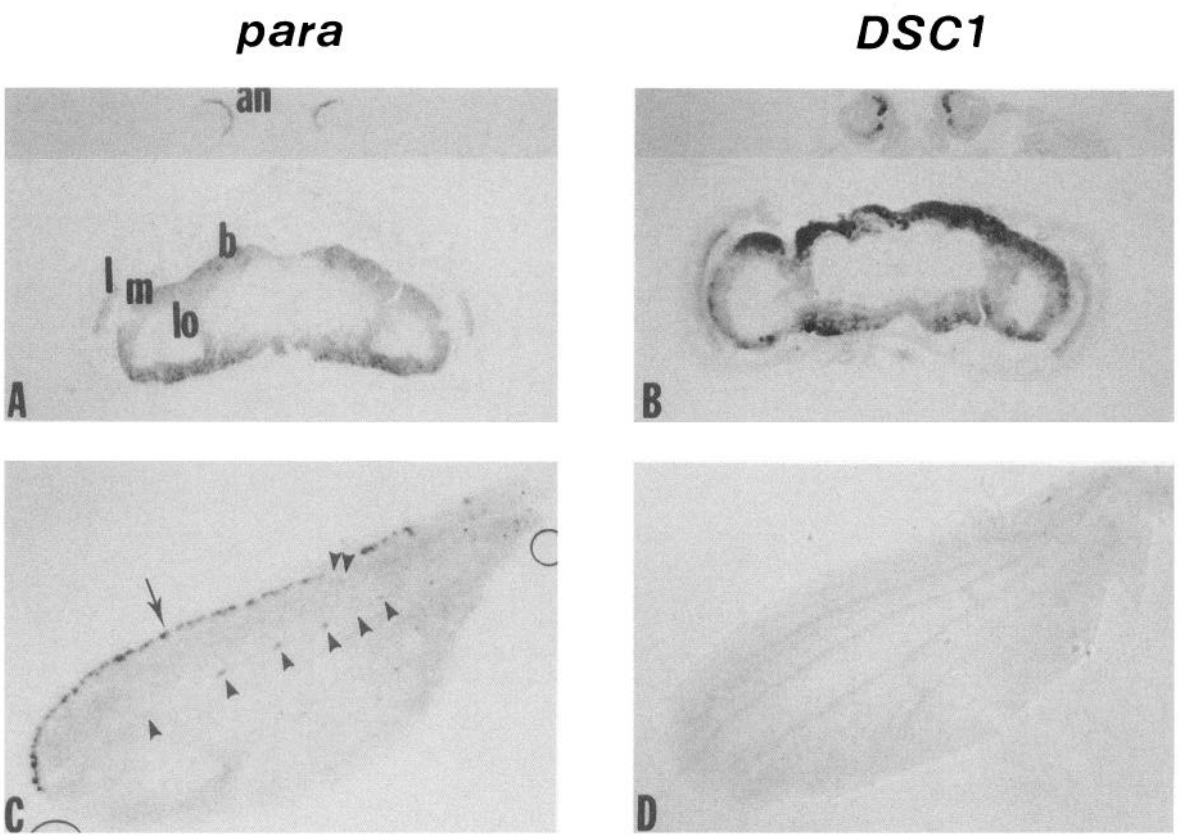

Figure 4. Expression of *para* and *DSC1* in 25 hr pupae. *A* and *C* show *para* expression, and *B* and *D*, *DSC1* expression. *A* and *B* are horizontal sections through the middle of pupal heads. Anterior is up. *A, In situ* hybridization with *para* probe. Staining appears over the cortical region of brain (*b*), lamina (*l*), medulla (*m*), lobular complex (*lo*), and also antennal neurons (*an*). *B, In situ* hybridization with *DSC1* probe. The pattern of *DSC1* expression appears to overlap with *para*. *C* and *D* show whole-mounts of pupal wings hybridized with *para* or *DSC1* probes. *C, para* probe. Note expression of *para* in the campaniform sensilla (*arrowheads*) along the third wing vein as well as in the sensory neurons along the anterior wing margin (*arrow*). *D, DSC1* probe. No expression of *DSC1* is detected in sensory neurons of pupal wings.

when the retina grows rapidly in length and undergoes final differentiation (Cagan and Ready, 1989), expression of *para* in this region becomes apparent (Fig. 5*A*; see also below).

In contrast to the limited expression of *DSC1* in embryos and larvae, its expression undergoes a substantial change beginning at the pupal stage. By 25 hr after pupariation, *DSC1* expression becomes prominent in the CNS and does not differ noticeably from that of *para* in the brain and optic regions (Fig. 4*B*). At this stage, *DSC1* is also expressed in antennal neurons in a pattern similar to *para*.

However, the expression of *para* and *DSC1* is still distinctive in some sensory neurons of the PNS such as in the developing pupal wing (Fig. 4*C,D*). A small array of well-defined sensory neurons is present in the developing wing 25 hr after pupariation (Murray et al., 1984). These include sensory neurons along the anterior margin of the wing and a group of eight campaniform sensilla along the third wing vein. All the marginal sensory neurons and all eight campaniform sensilla clearly express *para* (Fig. 4*C*). However, *DSC1* expression is not detected in any of these sensory neurons (Fig. 4*D*).

Expression of para *and* DSC1 *converges in late pupae and adults*

In 72 hr pupae and adults, *para* and *DSC1* transcripts are both present throughout the brain and thoracic ganglion (Fig. 5). Both transcripts are detected in the cortices of the lamina, medulla, and lobula complex as well as in the retina (Fig. 5*A,B,E,F*). Expression of both genes was detected in the retina in layers corresponding to the positions of the cell bodies of photoreceptors R1–R6, R7 and R8 (Fig. 5*G,H*). The neurons associated with the mechanosensory bristles of the eye also express both *para* and *DSC1*. Thus, in contrast with the distinct expression patterns of *para* and *DSC1* observed in earlier developmental stages, in late pupae and adults the expression of these two genes appears to be largely coextensive. Furthermore, from the pupal through adult stages, the intensity of the *DSC1* signal is reproducibly somewhat greater than that of *para*, suggesting that *DSC1* may be expressed at higher levels than *para* during these stages.

Discussion

We have examined the spatial and temporal expression of two *Drosophila* sodium channel genes, *para* and *DSC1*, in embryonic through adult stages. The *para* locus appears to encode the predominant class of sodium channels that is expressed ubiquitously in neurons of the CNS and PNS during all developmental stages. These results are in good agreement with conclusions based on previous genetic and electrophysiological analysis of *para* mutants. Homozygotes for *para* null mutations have an unconditionally recessive lethal phenotype and die as first instar larvae (B. Ganetzky, unpublished observations). Temperature-sensitive alleles, such as $para^{ts1}$, cause rapid pa-

ralysis of both larvae and adults at the restrictive temperature, as a result of a temperature-dependent block in the propagation of action potentials (Suzuki et al., 1971; Siddiqi and Benzer, 1976; Wu and Ganetzky, 1980; Benshalom and Dagan, 1981). Thus, it is likely that most, if not all, neurons require *para* expression for normal membrane excitability.

Despite the expression of *para* in most neurons, these neurons may not all express identical *para* polypeptides. The *para* transcript has been shown to undergo extensive alternative splicing and at least 18 different coding sequences have been detected *in vivo* (Loughney et al., 1989; Thackeray and Ganetzky, 1994). Furthermore, the relative frequencies of the various splice forms differ in embryos and adults (Thackeray and Ganetzky, 1994). Thus, temporal as well as spatial differences in splicing of the *para* transcript may contribute to the distinctive properties of different neurons. Differential distribution in the nervous system of splice variants from the *Sh* potassium channel locus has previously been reported in *Drosophila* (Schwarz et al., 1990).

Although *DSC1* also appears to encode a sodium channel polypeptide (Salkoff et al., 1987), its expression pattern is distinct from that of *para*. In embryos, only a small number of cells have detectable *DSC1* expression. In addition, most of the *DSC1*-positive cells are not detected by a neural-specific antibody. It may be that the *DSC1*-expressing cells in the embryonic ventral nerve cord correspond to longitudinal glial cells. The cells in the PNS ventral to the chordotonal organs that express *DSC1* may also be some type of non-neuronal supporting cell that has so far not been identified. Vertebrate glial cells in the PNS and CNS are known to express voltage-gated ion channels including sodium channels (Gautron et al., 1992; Ritchie, 1992). If the embryonic expression of *DSC1* is mostly limited to a few non-neuronal cells, this would explain why cultured neurons from embryos homozygous for a *DSC1* deletion expressed sodium currents of normal amplitude (Germeraad et al., 1992).

The failure to detect significant levels of *DSC1* expression in embryonic neurons does raise one puzzle. Egg hatch studies have shown that *para* null embryos survive through the completion of embryogenesis and up to 50% of these embryos hatch from the egg (Ganetzky, unpublished results). The larvae that emerge are extremely sluggish, fail to molt, and eventually die. Yet, the fact that a significant fraction manage to hatch indicates that *para* null larvae are able to perform the motor activity required to get out of the egg case. Injection of tetrodotoxin in mature embryos blocks the peristaltic contractions required for hatching, indicating that propagation of sodium channel–dependent action potentials is necessary to produce these movements (Keshishian et al., 1993). Analysis of null embryos produced by females that are germline mosaics for a *para* null allele (Ganetzky, unpublished results) and the *in situ* data reported here eliminate the possibility of maternally contributed *para* transcripts. Thus, one possible explanation for the ability of *para* null embryos to hatch is that sodium channels encoded by another gene provide the necessary function. A priori, *DSC1* appeared to be the most plausible candidate to fulfill such a role. However, this interpretation now appears unlikely on the basis of the embryonic *DSC1* expression pattern found here. Instead, we suggest the possible existence of at least one other sodium channel structural gene in *Drosophila* that is expressed in embryos. It will be of interest to try to identify this postulated gene.

Expression of *para* in the CNS of embryos and larvae indicates that it is transcribed in neurons but not in neuroblasts or ganglion mother cells. Thus, *para* does not appear to be expressed in these cells before they begin to become electrically active. Nonetheless, expression of *para* can be detected in photoreceptors of the developing eye disc. By this stage, the neuronal identity of these cells has already been specified (Venkatesh et al., 1985), although it is unclear whether they have yet become electrically active. Transcription of *para* in these cells wanes as the ommatidial cluster matures such that very little or no *para* expression is detected in the most posterior region of the eye disc. Furthermore, no significant expression of *para* could be detected in photoreceptors of 25 hr pupae. Thus, it appears that there is a very short period of *para* expression during the early differentiation of photoreceptor cells. Subsequently, expression of *para* is reduced or absent in these cells until late pupal stages when strong expression resumes. Although both *para* and *DSC1* are expressed in photoreceptors of late pupae, only *para* is expressed in the developing eye disc. To examine the potential significance of *para* expression in the developing eye disc, we generated mosaic patches homozygous for a *para* null mutation. However, this elimination of *para* expression in the eye disc did not cause any gross abnormalities in development of the retina or in any of the downstream optic ganglia. Whether there might be more subtle defects in these mosaic patches, such as perturbation of axonal pathfinding, has not been examined.

Aside from the question of early *para* expression in the eye disc, expression of both *para* and *DSC1* transcripts in fully mature photoreceptors was unexpected. In *Diptera*, as in other insects, transmission of the receptor signal down the retinula cell axon to the synaptic ending is thought to depend on passive spread of the receptor potential (Pak and Grabowki, 1978). Intracellular recordings from dipteran photoreceptors have never indicated the occurrence of action potentials (Pak and Grabowski, 1978). Furthermore, the presence of voltage-activated sodium channels was not evident in whole-cell patch-clamp recordings of dissociated *Drosophila* photoreceptors (Hardie, 1991). However, voltage-activated sodium channels have been found in photoreceptors of drone honeybees where they are involved in the amplification of small signals (Vallet et al., 1992). Because drone photoreceptors have evolved for the effective performance a specific task—detection of spots in the sky that might be queen bees—it is not clear whether a comparable amplification mechanism occurs, or is required, in *Drosophila*. Thus, the role of sodium channels in the development and function of *Drosophila* photoreceptors is an interesting question for further study.

In pupae and adults, expression of *para* and *DSC1* remains different in the PNS but overlaps almost completely in the CNS. An important neuronal function for *DSC1* is suggested by its strong and widespread expression in the pupal and adult CNS. Why do most, if not all, CNS neurons express two sodium channel genes? Because the polypeptides encoded by *para* and *DSC1* are quite distinct and have probably been diverging from each other for at least 600 million years, they may have different properties enabling them to subserve different physiological functions—a conclusion supported by the results of gene dosage studies (Stern et al., 1990). For example, a single neuron could express two types of sodium channels, one targeted for axons and one for cell bodies or terminals. Distribution to different functional domains has been demonstrated for two members of the *Sh* family of potassium channels in hippocampal neurons (Sheng et al., 1992). Determination of the subcellular distribution of *para* and *DSC1* polypeptides with type-specific antibodies would be informative in this regard. On the other hand,

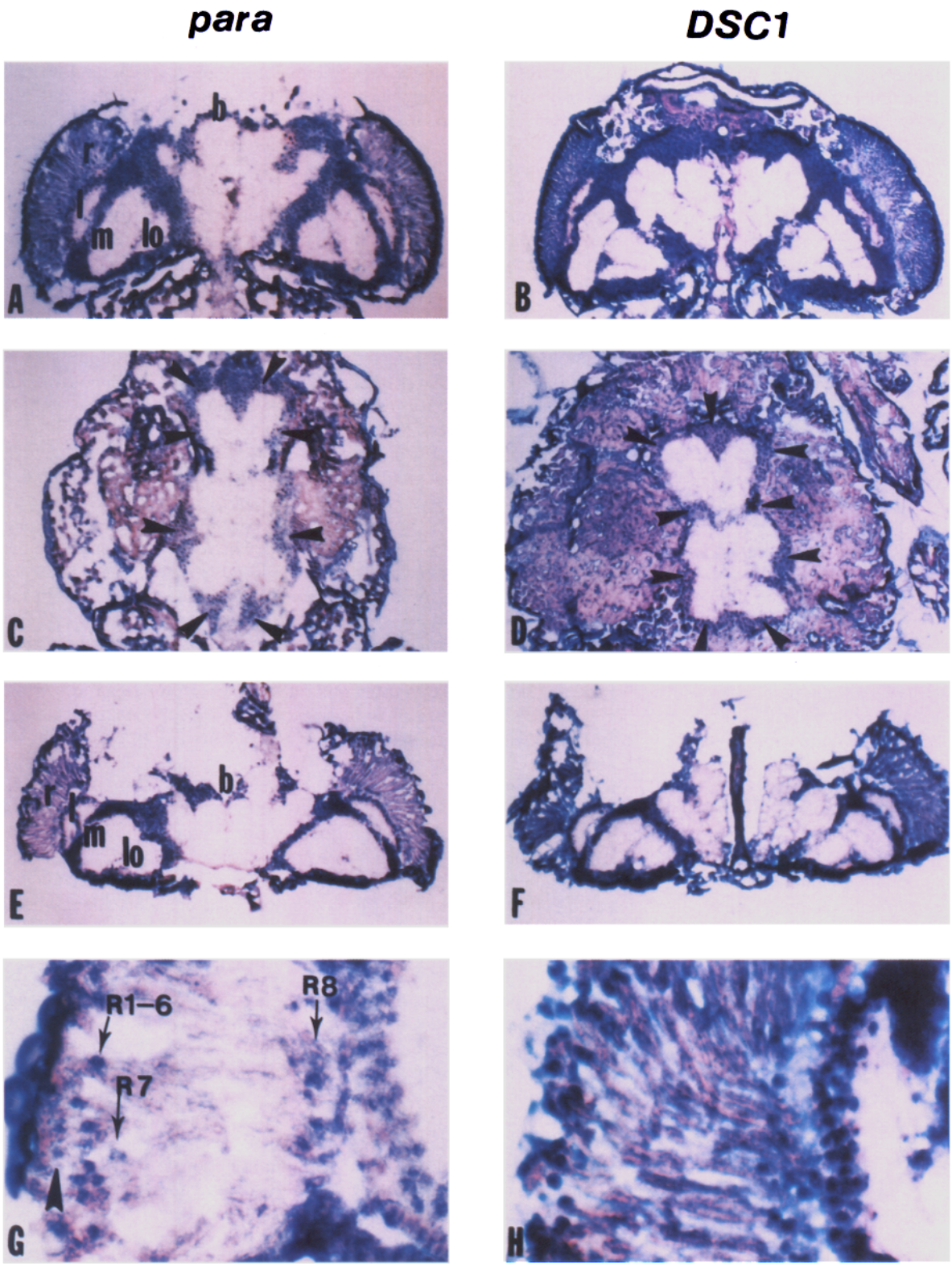

Figure 5. Expression of *para* and *DSC1* in 72 hr pupae and in adult heads. *Left panels* (*A, C, E,* and *G*) show *para* expression, and *right panels* (*B, D, F,* and *H*), *DSC1* expression. *A* and *B* are horizontal sections through the middle of pupal heads. *C* and *D* are horizontal sections through the middle of thoraces. *E–H* are horizontal sections through the middle of adult heads about 4 d after eclosion. Anterior is up. *A,* Hybridization with *para* probe. *B,* Hybridization with *DSC1* probe. Expression of both *para* and *DSC1* can be detected in cellular cortices of brain (*b*), retina (*r*), lamina (*l*), medulla (*m*), and the lobular complex (*lo*). Note that expression in the retina is detected in 72 hr pupae, although it was absent earlier in 25 hr pupae. *C,* Hybridization with *para* probe. *D,* Hybridization with *DSC1* probe. Both *para* and *DSC1* are expressed in the cellular cortex of thoracic ganglion (*arrowheads*) but neither gene has detectable expression in cells outside the nervous system. *E,* Hybridization with *para* probe. *F,* Hybridization with *DSC1* probe. For both *para* and *DSC1* the staining pattern in the cellular cortices of brain (*b*), retina (*r*), lamina (*l*), medulla (*m*), and lobular complex (*lo*) are all the same as in late pupal stages. *G* and *H* show a higher magnification of the retinal region. *G,* Hybridization with *para* probe. *H,* Hybridization with *DSC1* probe. The photoreceptors, R8 and R7 as well as R1–R6 located in a layer just distal to R7 are all stained. The sensory neurons of the eye bristle (*arrowhead*) close to the photoreceptors R1–R6 seems to be stained.

some functional overlap between *para* and *DSC1* could help explain the persistence of action potentials in neurons of the flight motor pathway in $para^{ts}$ adults at restrictive temperatures (Elkins and Ganetzky, 1990). Isolation of *DSC1* mutations would be very useful in addressing its functional role *in vivo*.

References

Amichot M, Castella C, Berge JB, Pauron D (1993) Transcription analysis of the *para* gene by *in situ* hybridization and immunological characterization of its expression product in wild-type and mutant strains of *Drosophila*. Insect Biochem Mol Biol 23:381–390.

Benshalom G, Dagan D (1981) Electrophysiological analysis of the temperature-sensitive paralytic *Drosophila* mutant, $para^{ts}$. J Comp Physiol 144:409–417.

Cagan RL, Ready DF (1989) The emergence of order in the *Drosophila* pupal retina. Dev Biol 136:346–362.

Campos-Ortega JA, Hartenstein V (1985) Stages of *Drosophila* embryogenesis. In: The embryonic development of *Drosophila melanogaster*, pp 9–84. New York: Springer.

Campos-Ortega JA, Jan YN (1991) Genetic and molecular bases of neurogenesis in *Drosophila melanogaster*. Annu Rev Neurosci 14: 399–420.

Elkins T, Ganetzky B (1990) Conduction in the giant nerve fiber pathway in temperature-sensitive paralytic mutants of *Drosophila*. J Neurogenet 6:207–219.

Gautron S, Santos GD, Pinto-Henrique D, Koulakoff A, Gros F, Berwald-Netter Y (1992) The glial voltage-gated sodium channel: cell- and tissue-specific mRNA expression. Proc Natl Acad Sci USA 89: 7272–7276.

Germeraad S, O'Dowd DK, Aldrich RW (1992) Functional assay of a putative *Drosophila* sodium channel gene in homozygous deficiency neurons. J Neurogenet 8:1–16.

Hafen E, Levine M (1986) The localization of RNAs in *Drosophila* tissue sections by *in situ* hybridization. In: *Drosophila*, a practical approach (Roberts DB, ed), pp 139–157. Oxford: IRL.

Hardie RC (1991) Voltage-sensitive potassium channels in *Drosophila* photoreceptors. J Neurosci 11:3079–3095.

Hartenstein V (1988) Development of *Drosophila* larval organs: spatiotemporal pattern of sensory neurons, peripheral axonal pathways and sensilla differentiation. Development 102:869–886.

Hille B (1992) Ion channels of excitable membranes, 2d ed. Sunderland, MA: Sinauer.

Huang F, Dambly-Chaudiere C, Ghysen A (1991) The emergence of sense organs in the wing disc of *Drosophila*. Development 111:1087–1095.

Jan LY, Jan YN (1982) Antibodies to horseradish peroxidase as specific neuronal markers in *Drosophila* and in grasshopper embryos. Proc Natl Acad Sci USA 72:2700–2704.

Jan YN, Ghysen A, Christoph I, Barbel S, Jan LY (1985) Formation of neuronal pathways in the imaginal discs of *Drosophila melanogaster*. J Neurosci 5:2453–2464.

Kallen RG, Sheng Z-H, Yang J, Chen L, Rogart RB, Barchi RL (1990) Primary structure and expression of a sodium channel characteristic of denervated and immature rat skeletal muscle. Neuron 4:233–242.

Kankel DR, Ferrus A, Garen SH, Harte PJ, Lewis PE (1980) The structure and development of the nervous system. In: The genetics and biology of *Drosophila*, Vol 2d (Ashburner M, Wright TRF, eds), pp 295–368. New York: Academic.

Kayano T, Noda M, Flockerzi V, Takahashi H, Numa S (1988) Primary structure of rat brain sodium channel III deduced from the cDNA sequence. FEBS Lett 228:187–194.

Keshishian H, Chiba A, Chang TN, Halfon MS, Harkins EW, Jarecki J, Wang L, Anderson M, Cash S, Halpern ME, Johansen J (1993) Cellular mechanisms governing synaptic development in *Drosophila melanogaster*. J Neurobiol 24:757–787.

Klambt C, Goodman CS (1991) The diversity and pattern of glia during axon pathway formation in the *Drosophila* embryo. Glia 4:205–213.

Loughney K, Kreber R, Ganetzky B (1989) Molecular analysis of the *para* locus a sodium channel gene in *Drosophila*. Cell 58:1143–1154.

Mandel G (1992) Tissue-specific expression of the voltage sensitive sodium channel. J Membr Biol 125:193–205.

Masucci JD, Miltenberger RJ, Hoffmann FM (1990) Pattern-specific expression of the *Drosophila decapentaplegic* gene in imaginal disks is regulated by 3′ cis-regulatory elements. Genes Dev 4:2011–2023.

Murray MA, Schubiger M, Palka J (1984) Neuron differentiation and axon growth in the developing wing of *Drosophila melanogaster*. Dev Biol 104:259–273.

Noda M, Ikeda T, Kayano T, Suzuki H, Takeshima H, Kurasaki M, Takahashi H, Numa S (1986) Existence of distinct sodium channel messenger RNAs in rat brain. Nature 320:188–192.

Pak WL, Grabowski SR (1978) Physiology of the visual and flight systems. In: The genetics and biology of *Drosophila*, Vol 2a (Ashburner M, Wright TRF, eds), pp 553–604. New York: Academic.

Ramaswami M, Tanouye M (1989) Two sodium channel genes in *Drosophila*: implications for channel diversity. Proc Natl Acad Sci USA 86:2079–2082.

Ready DF, Hanson TE, Benzer S (1976) Development of the *Drosophila* retina, a neurocrystalline lattice. Dev Biol 53:217–240.

Reuter R, Scott MP (1990) Expression and function of the homoetic genes *Antennapedia* and *Sex combs reduced* in the embryonic midgut of *Drosophila*. Development 109:289–303.

Ritchie JM (1992) Voltage-gated ion channels in Schwann cells and glia. Trends Neurosci 15:345–350.

Rogart RB, Cribbs LL, Muglia LK, Kephart DD, Kaiser MW (1989) Molecular cloning of a putative tetrodotoxin-resistant rat heart Na^+ channel isoform. Proc Natl Acad Sci USA 86:8170–8174.

Salkoff L, Butler A, Wei A, Scavarda N, Giffen K, Ifune C, Goodman R, Mandel G (1987) Genomic organization and deduced amino acid sequence of a putative sodium channel gene in *Drosophila*. Science 237:744–749.

Schwarz TL, Papazian DM, Carretto RC, Jan YN, Jan LY (1990) Immunological characterization of K^+ channel components from the *Shaker* locus and differential distribution of splicing variants in *Drosophila*. Neuron 2:119–127.

Sheng M, Tsaur M, Jan YN, Jan LY (1992) Subcellular segregation of two A-type K^+ channel proteins in rat central neurons. Neuron 9:271–284.

Siddiqi O, Benzer S (1976) Neurophysiological defects in temperature-sensitive mutants of *Drosophila melanogaster*. Proc Natl Acad Sci USA 73:3253–3257.

Stern M, Kreber R, Ganetzky B (1990) Dosage effects of a *Drosophila* sodium channel gene on behavior and axonal excitability. Genetics 124:133–143.

Suzuki DT, Grigliatti T, Williamson R (1971) Temperature-sensitive mutations in *Drosophila melanogaster*, VII. A mutation ($para^{ts}$) causing reversible adult paralysis. Proc Natl Acad Sci USA 68:890–893.

Tautz D, Pfeifle C (1989) A non-radioactive *in situ* hybridization method for the localization of specific RNAs in *Drosophila* embryos reveals translational control of the segmentation gene *hunchback*. Chromosoma 98:81–85.

Thackeray JR, Ganetzky B (1994) Developmentally regulated alternative splicing generates a complex array of *Drosophila para* sodium channel isoforms. J Neurosci 14:2569–2578.

Tix S, Bate M, Technau GM (1989) Pre-existing neuronal pathways in the leg imaginal discs of *Drosophila*. Development 107:855–862.

Trimmer JS, Cooperman SS, Tomiko SA, Zhou J, Crean SM, Boyle MB, Kallen RG, Sheng Z, Barchi RL, Sigworth FJ, Goodman RH, Agnew WS, Mandel G (1989) Primary structure and functional expression of a mammalian skeletal muscle sodium channel. Neuron 3:33–49.

Truman J, Bate M (1988) Spatial and temporal patterns of neurogenesis in the central nervous system of *Drosophila melanogaster*. Dev Biol 125:145–157.

Tseng-Crank J, Pollock JA, Hayashi I, Tanouye MA (1991) Expression of ion channel genes in *Drosophila*. J Neurogenet 7:229–239.

Vallet AM, Coles JA, Eilbeck JC, Scott AC (1992) Membrane conductances involved in amplification of small signals by sodium channels in photoreceptors of drone honey bee. J Physiol (Lond) 456:303–324.

Venkatesh TR, Zipursky SL, Benzer S (1985) Molecular analysis of the development of the compound eye in *Drosophila*. Trends Neurosci 8:251–257.

White K, Kankel DR (1978) Patterns of cell division and cell movement in the formation of the imaginal nervous system in *Drosophila melanogaster*. Dev Biol 65:296–321.

Wu C-F, Ganetzky B (1980) Genetic alteration of nerve membrane excitability in temperature-sensitive paralytic mutants of *Drosophila melanogaster*. Nature 286:814–816.